Chromium–Niobium Co-Doped Vanadium Dioxide Films: Large Temperature Coefficient of Resistance and Practically No Thermal Hysteresis of the Metal–Insulator Transition*

Kenichi MIYAZAKI **Keisuke SHIBUYA** **Megumi SUZUKI**
Kenichi SAKAI **Jun-ichi FUJITA, and Akihito SAWA**

We investigated the effects of chromium (Cr) and niobium (Nb) co-doping on the temperature coefficient of resistance (TCR) and the thermal hysteresis of the metal–insulator transition of vanadium dioxide (VO_2) films. We determined the TCR and thermal-hysteresis-width diagram of the $V_{1-x-y}Cr_xNb_yO_2$ films by electrical-transport measurements and we found that the doping conditions $x \gtrsim y$ and $x + y \geq 0.1$ are appropriate for simultaneously realizing a large TCR value and an absence of thermal hysteresis in the films. By using these findings, we developed a $V_{0.90}Cr_{0.06}Nb_{0.04}O_2$ film grown on a TiO_2-buffered SiO_2/Si substrate that showed practically no thermal hysteresis while retaining a large TCR of 11.9%/K. This study has potential applications in the development of VO_2-based uncooled bolometers.

Key words :
bolometer, VO_2, metal-insulator transition, co-doping, TCR.

1. INTRODUCTION

Vanadium oxides exhibit a temperature-induced metal–insulator transition (MIT) with a discontinuous change in electrical conductivity of several orders of magnitude[1]. The MIT is the first-order structural transition and is also accompanied by a marked change in the optical transmittance in the infrared (IR) region. Among the various oxides of vanadium, vanadium dioxide (VO_2) is the most interesting from an application perspective because its MIT occurs at around 340 K, which is above room temperature[2]. An MIT above room temperature is useful in a variety of functional devices, such as electrical switches, gas sensors, smart windows, uncooled bolometers, or thermal memories[3]. Among these devices, VO_2-based uncooled bolometers that detect far-IR radiation have been actively studied and developed for several decades[4–8].

One measure of the suitability of a material for use in

基盤技術

＊ AIP advances 6, 055012 (2016) より転載。

a bolometer is its temperature coefficient of resistance (TCR), which is defined as $|(1/\rho)(d\rho/dT)|$, where ρ is the resistivity or resistance and T is the temperature of the material. The TCR value of VO_2 reaches more than 70%/K near the MIT temperature (T_{MI})[9], which is more than ten times that of conventional uncooled bolometer materials such as Si or Ge.[10–12] However, VO_2 shows a large thermal hysteresis in the ρ–T curve across the MIT. The hysteretic behavior indicates the coexistence of two phases over a finite temperature range due to superheating and supercooling effects, which is a characteristic of the first-order transition. The thermal hysteresis in the ρ–T curve results in poor measurement reproducibility in IR sensing. Consequently, thermal hysteresis has to be minimized to realize high-sensitivity uncooled bolometers based on VO_2.

Doping of VO_2 with metal ions has been employed as a means of suppressing its thermal hysteresis;[13,14] however, doping with metal ions also gives rise to a reduction in the TCR of VO_2. We previously conducted a systematic study of the TCR and thermal hysteresis in VO_2 doped with Cr or with Nb, and we found that there is a correlation between the TCR and thermal hysteresis, which is independent of the doping element[15]. Our findings implied that a high TCR and the absence of thermal hysteresis were difficult to achieve simultaneously in single-element doped VO_2. However, Soltani *et al.* reported that co-doping of VO_2 with Ti and W suppresses thermal hysteresis more effectively than does doping with W alone[16]. In their study, they simultaneously achieved a practical absence of thermal hysteresis and a TCR of 5.12%/K at room temperature in $V_{0.866}W_{0.014}Ti_{0.12}O_2$ films. This TCR is larger than that of conventional uncooled bolometer materials. However, it is still challenging to achieve the high TCR values in excess of 10%/K that are required for high-sensitivity uncooled bolometers.

In this study, we explored the possibility of obtaining high TCR values with no thermal hysteresis by co-doping VO_2 films with Cr and Nb. Note that V, Cr, and Nb ions are tetravalent (4+), trivalent (3+), and pentavalent (5+), respectively, and that their effective radii are 0.058, 0.062, and 0.064 nm, respectively. We previously reported that Nb doping is effective in reducing the thermal hysteresis of VO_2;[15] however, it also causes a rapid decrease in its TCR. In contrast, the decrease in the TCR of VO_2 on doping with Cr is moderate, but Cr doping is less effective than Nb doping in reducing the thermal hysteresis. These differing effects on the TCR and thermal hysteresis might be due to the differences in the valence states and/or ionic radii of the Cr and Nb ions[15]. Because Cr and Nb dopants are effective in maintaining large TCR values and in reducing the thermal hysteresis, respectively, co-doping with Cr and Nb might give rise to a combination of the desirable effects of the two individual ions.

From ρ–T measurements on the $V_{1-x-y}Cr_xNb_yO_2$ films, we derived a TCR and thermal-hysteresis-width (ΔT_{MI}) diagram for the films. This diagram revealed that doping conditions of $x \gtrsim y$ and $x + y \geq 0.1$ are suitable for producing films that show no thermal hysteresis while retaining a large TCR. We also succeeded in producing a large TCR of 11.9%/K and practically no thermal hysteresis in $V_{0.90}Cr_{0.06}Nb_{0.04}O_2$ films fabricated on TiO_2-buffered SiO_2/Si substrates at process temperatures below 670 K.

2. EXPERIMENTAL

$V_{1-x-y}Cr_xNb_yO_2$ films were grown on α-Al_2O_3 (0001) single-crystal substrates and TiO_2/SiO_2/Si (100) substrates by pulsed-laser deposition with a KrF excimer laser (λ = 248 nm). Mixed ceramic pellets consisting of V_2O_5, Cr_2O_3, and Nb_2O_5 were used as targets. The doping range for Cr was x = 0–0.12 and that of Nb was y = 0–0.09. We have previously described the detailed conditions for growth of such films on Al_2O_3[15] or $TiO_2/SiO_2/Si$ substrates[17]. The film thickness was set at 70–110 nm, as confirmed by using a surface profiler. Note that there were no significant differences in the structural or electronic properties of the films within this thickness range. The resistivity of the films was measured by conventional four-probe methods using Ti/Au electrodes. Transport properties were examined by using a physical property measurement system (PPMS; Quantum Design), and the temperature sweep rate was set to 0.3 K/min.

3. RESULTS AND DISCUSSIONS

Fig. 1(a) and **Fig. 1(b)** show the ρ–T curves for the $V_{0.95-x}Cr_xNb_{0.05}O_2$ and $V_{0.95-y}Cr_{0.05}Nb_yO_2$ films on Al_2O_3 substrates with $0 \le x \le 0.12$ and $0 \le y \le 0.08$, respectively. As a reference, the ρ–T curve for a nondoped VO_2 film is also shown in **Fig. 1(b)**. A systematic change in T_{MI} with doping was observed. Here, T_{MI} is defined as the halfway point between the temperatures of the two peaks in the TCR for the heating and cooling processes, respectively. In addition to the change in T_{MI}, the doping affected the values of the TCR and ΔT_{MI}. The co-doped films showed a broadening of the MIT, and the change in ρ across the MIT for the co-doped films was smaller than that for the nondoped film. These behaviors caused a decrease in the TCR of the co-doped films. Moreover, the co-doped films had a smaller ΔT_{MI} compared with the nondoped film.

Fig. 2(a) and **Fig. 2(b)** show the dependence of T_{MI}, the maximum TCR, and ΔT_{MI} on the total dopant content $x + y$ for the $V_{0.95-x}Cr_xNb_{0.05}O_2$ and $V_{0.95-y}Cr_{0.05}Nb_yO_2$ films on Al_2O_3 substrates, respectively. The results of single-element doping[16] are also plotted for comparison. It is well known that hole doping by lower-valence elements such as Cr^{3+} or Al^{3+} raises the T_{MI}, whereas electron doping with higher-valence elements such as Nb^{5+} or W^{6+} lowers the T_{MI}[15,18-20]. These tendencies are maintained in co-doped VO_2. As seen in the top panels in **Fig. 2**, an increase in the Cr content raised the T_{MI} of the $V_{0.95-x}Cr_xNb_{0.05}O_2$ films, whereas an increase in the Nb content reduced

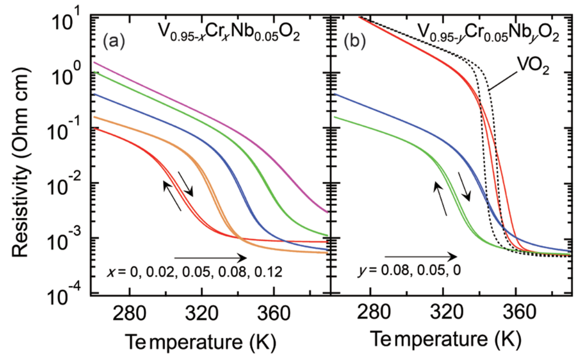

Fig. 1 Temperature dependence of the resistivity of (a) $V_{0.95-x}Cr_xNb_{0.05}O_2$ and (b) $V_{0.95-y}Cr_{0.05}Nb_yO_2$ films. As a reference, the ρ–T curve for the nondoped VO_2 film (dashed line) is plotted in (b).

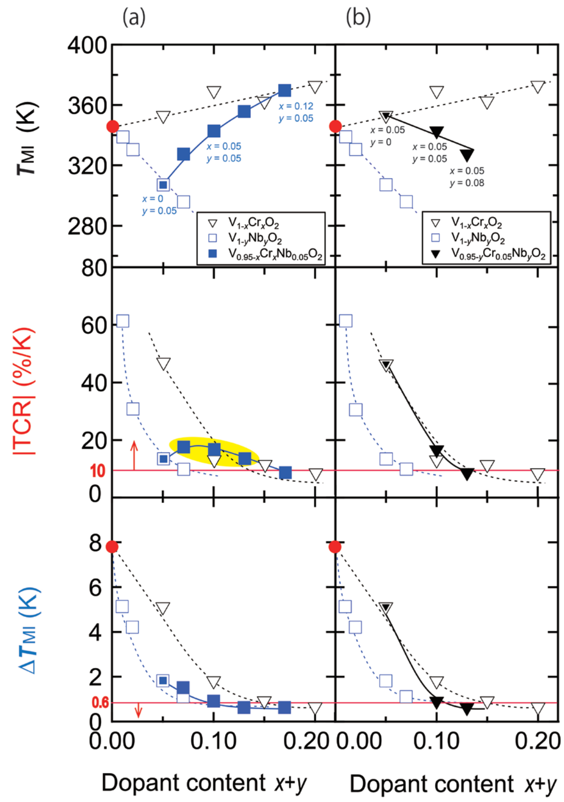

Fig. 2 Cr content (x) and Nb content (y) dependence of T_{MI}, TCR, and ΔT_{MI} for (a) $V_{0.95-x}Cr_xNb_{0.05}O_2$ and (b) $V_{0.95-y}Cr_{0.05}Nb_yO_2$ films. An increase in the TCR in the $V_{0.95-x}Cr_xNb_{0.05}O_2$ (x = 0.02, 0.05, and 0.08) films with respect to that of the $V_{0.95}Nb_{0.05}O_2$ (x = 0) film is highlighted.

基盤技術

the T_{MI} of the $V_{0.95-y}Cr_{0.05}Nb_yO_2$ films. The T_{MI} of the $V_{0.90}Cr_{0.05}Nb_{0.05}O_2$ ($x = y = 0.05$) film was almost identical to that of the nondoped VO_2 film. These results can be explained in terms of the valence state A+ of the V ions, which can be defined as $A = 4 + x - y$. The T_{MI} of the co-doped films is dominated by the valence state of the V ions.

Doping of VO_2 with metal ions generally induces a broadening of the MIT, resulting in a decrease in the TCR. This behavior can be understood in terms of a spatial variation in the T_{MI}, attributable to an inhomogeneity of the carrier concentration and to lattice deformation and/or defects[21,22]. As shown in the middle panels in **Fig. 2**, for single-element doping with Cr or Nb, the maximum TCR decreased monotonically with increasing dopant content, with Nb doping having the greater effect. In contrast to single-element doping, co-doped $V_{0.95-x}Cr_xNb_{0.05}O_2$ films showed a nonmonotonic decrease with increasing x. The $V_{0.95-x}Cr_xNb_{0.05}O_2$ films with $x = 0.02$, 0.05, and 0.08 had larger TCR values than that of the $V_{0.95}Nb_{0.05}O_2$ film ($x = 0$), as highlighted in the middle panel in **Fig. 2(a)**. For $x \geq 0.05$ ($= y$), the $x + y$ dependence of the TCR values for the $V_{0.95-x}Cr_xNb_{0.05}O_2$ films is almost coincident with that for the $V_{1-x}Cr_xO_2$ films. This behavior can be also seen in the $V_{0.95-y}Cr_{0.05}Nb_yO_2$ films [the middle panel of **Fig. 2(b)**]. These results suggest that the presence of Cr dopant with the condition $x \gtrsim y$ is essential for obtaining large TCR values in $V_{1-x-y}Cr_xNb_yO_2$ films.

The bottom panels in **Fig. 2** show that for single-element doping, ΔT_{MI} also decreases monotonically with increasing dopant content and that it is reduced more efficiently by doping with Nb than with Cr. Note that the ΔT_{MI} is defined as the difference in the temperatures at which a film has a given resistivity (ρ_{MI}) during the heating and cooling phases. For this study, we choose ρ_{MI} as the value of ρ at the temperature of the TCR peak in the heating process[15]. In contrast to the TCR value, the $x + y$ dependence of ΔT_{MI} for both $V_{0.95-x}Cr_xNb_{0.05}O_2$ and $V_{0.95-y}Cr_{0.05}Nb_yO_2$ films approached that of $V_{1-y}Nb_yO_2$ films. This result suggests that the presence of Nb dopant is essential for effectively reducing the ΔT_{MI} with the minimum possible dopant content. Moreover, to realize a near absence of thermal hysteresis (defined as $\Delta T_{MI} \leq 0.6$ K), a dopant content of $x + y \geq 0.1$ is required.

We therefore found that co-doping of VO_2 with Cr and Nb is an effective means of suppressing thermal hysteresis (i.e., ΔT_{MI}) while retaining a large TCR. For $V_{1-x-y}Cr_xNb_yO_2$ films, the conditions $x \gtrsim y$ and $x + y \geq 0.1$ are essential for obtaining large TCR values in excess of 10%/K and a near absence of thermal hysteresis ($\Delta T_{MI} \leq 0.6$ K), respectively. As seen in **Fig. 2(a)**, large TCR values of 16.7%/K with a $\Delta T_{MI} \approx 0.9$ K or 13.6%/K with $\Delta T_{MI} \approx 0.6$ K were attained with $V_{0.90}Cr_{0.05}Nb_{0.05}O_2$ ($x = 0.05$, $y = 0.05$) and $V_{0.87}Cr_{0.08}Nb_{0.05}O_2$ ($x = 0.08$, $y = 0.05$) films, respectively.

To further explore the optimal composition of the doped films, we examined the dependence of TCR and ΔT_{MI} on x and y for $V_{1-x-y}Cr_xNb_yO_2$ films on Al_2O_3 substrates and we derived the diagram for the TCR and ΔT_{MI} of the $V_{1-x-y}Cr_xNb_yO_2$ films shown in **Fig. 3**. As x and y increase, the TCR value decreases monotonically. Relatively large TCR values were obtained near the line $x = y$. Furthermore, the TCR contour lines/domains are asymmetric with respect to this line. This asymmetry indicates that a condition of $x \gtrsim y$ is suitable for obtaining a large TCR for $V_{1-x-y}Cr_xNb_yO_2$ films, as mentioned earlier. In contrast to the TCR, ΔT_{MI} does not show a clear trend with x and y. However, the diagram confirms that a practical absence of thermal hysteresis can be obtained for co-doped $V_{1-x-y}Cr_xNb_yO_2$ films with $x + y \geq 0.1$. Therefore, because the total dopant content $x + y$ should be as small as possible to obtain a large TCR, the optimal composition can be expected to be near the line $x + y = 0.1$ with the condition $x \gtrsim y$, as shown by the solid circle in **Fig. 3**. In fact, among the films that showed practically no thermal hysteresis, the $V_{0.90}Cr_{0.06}Nb_{0.04}O_2$ film showed the best TCR of 16.2%/K.

Next, we will briefly discuss the effects of Cr and Nb co-doping on the MIT of VO_2. One of the important effects of Cr and Nb co-doping is that of charge compensation. Because Cr and Nb ions are trivalent and pentavalent, respectively, Cr and Nb co-doping of VO_2 has less overall effect on the change in the valence state of V^{4+} ions than does single-element doping. Therefore, any inhomogeneity of carrier concentration that results in a spatial variation in T_{MI} should be reduced in co-doped VO_2 films. As a result, broadening of the MIT is suppressed, leading to an improvement in the TCR of the co-doped films. However, because of the different ionic radii of V, Cr, and Nb ions, Cr and Nb co-doping still induces lattice deformations and defects in VO_2. We previously reported that Cr doping suppresses the lattice changes in VO_2 across the MIT that originate from a structural phase transition from a high-temperature tetragonal phase to a low-temperature monoclinic phase[15] .The suppression of this lattice change in the doped films might be the cause of the decrease in the TCR and ΔT_{MI}. Because different doping elements induce different low-temperature monoclinic phases in VO_2[18,19,23], the lattice change across the MIT in the co-doped films is expected to be more complicated than that in the single-element doped films. To gain a better understanding of the effects of co-doping on the TCR and ΔT_{MI}, detailed investigations of the structural properties of the co-doped VO_2 films are required, and will be a subject of a further study.

For uncooled bolometer applications, VO_2 films should be integrated onto Si platforms through a back-end-of-line (BEOL) process. We previously reported that TiO_2 buffer layers permit the fabrication

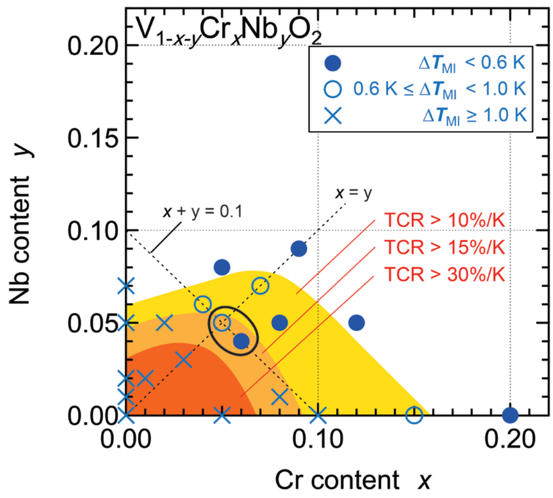

Fig. 3 TCR and ΔT_{MI} diagram for $V_{1-x-y}Cr_xNb_yO_2$ films as a function of the Cr and Nb contents. Values of ΔT_{MI} are divided into three categories: $\Delta T_{MI} \leq 0.6$ K (filled circles), $0.6\ K < \Delta T_{MI} \leq 1.0$ K (open circles), and $\Delta T_{MI} > 1.0$ K (crosses). The TCR values are classified into three regions: >10%/K, >15%/K, and >30%/K

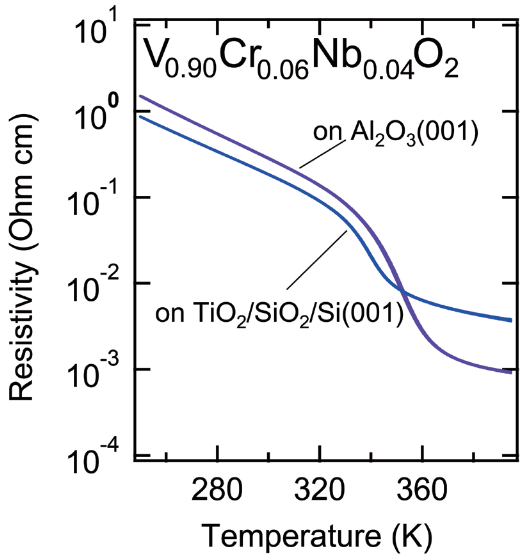

Fig. 4 Temperature dependence of the resistivity of $V_{0.90}Cr_{0.06}Nb_{0.04}O_2$ films on Al_2O_3 (0001) and $TiO_2/SiO_2/Si$ (100) substrates

of VO_2 films that show a sharp MIT on SiO_2/Si (100) substrates at process temperatures below 670 K, which is compatible with a BEOL process[17]. By using the TiO_2-buffer technique, we deposited $V_{1-x-y}Cr_xNb_yO_2$ films on SiO_2/Si (100) substrates to realize both large TCR values and an absence of thermal hysteresis. **Fig. 4** shows the ρ–T curves for the

基盤技術

$V_{0.90}Cr_{0.06}Nb_{0.04}O_2$ films on Al_2O_3 and $TiO_2/SiO_2/Si$ substrates. As mentioned earlier, the film on the Al_2O_3 substrate showed practically no thermal hysteresis while retaining a large TCR of 16.2%/K. On the other hand, the film on the $TiO_2/SiO_2/Si$ substrate showed a reduced ρ change across the MIT but retained a large TCR of 11.9%/K. This result suggests that a combination of co-doping and the TiO_2-buffer techniques provides an effective way of integrating a VO_2 film having large TCR values and a practical absence of thermal hysteresis on a Si platform.

4. SUMMARY

We have investigated the effects of co-doping of VO_2 with Cr and Nb on the TCR and the thermal hysteresis of the MIT, and we have derived a TCR and ΔT_{MI} diagram for $V_{1-x-y}Cr_xNb_yO_2$ films on Al_2O_3 substrates. The diagram showed that the doping conditions of $x \gtrsim y$ (i.e., a slightly Cr-rich condition) and $x + y \geq 0.1$ are suitable for simultaneously obtaining a large TCR and an absence of thermal hysteresis in the $V_{1-x-y}Cr_xNb_yO_2$ films. By employing Cr and Nb co-doping and the TiO_2-buffer technique, we succeeded in obtaining a large TCR value of 11.9%K with practically no thermal hysteresis in $V_{0.90}Cr_{0.06}Nb_{0.04}O_2$ films deposited on SiO_2/Si substrates at process temperatures below 670 K, which are compatible with a BEOL process. This combined technique might be applicable in the development of VO_2-based uncooled bolometers with a high sensitivity.

REFERENCES

1) F. J. Morin, Phys. Rev. Lett. 3, 34 (1959).
2) J. B. Goodenough, J. Solid State Chem. 3, 490 (1971).
3) Z. Yang, C. Ko, and S. Ramanathan, Annu. Rev. Mater. Res. 41, 337 (2011).
4) M. Soltani, M. Chaker, E. Haddad, R. Kruzelecky, and J. Margot, J. Vac. Sci. Technol. A 25, 971 (2007).
5) S. Bonora, U. Bortolozzo, S. Residori, R. Balu, and P. V. Ashrit, Opt. Lett. 35, 103 (2010).
6) Y. Gao, H. Luo, Z. Zhang, L. Kang, Z. Chen, J.Du, M. Kanehira, and C. Cao, Nano Energy 1, 221 (2012).
7) R. Xie, C. T. Bui, B. Varghese, Q. Zhang, C. H. Sow, B. Li, and J. T. L. Thong, Adv. Funct. Mater. 21, 1602 (2011).
8) M. Nakano, K. Shibuya, D. Okuyama, T. Hatano, S. Ono, M. Kawasaki, Y. Iwasa, and Y. Tokura, Nature 487, 459 (2012).
9) H. Takami, K. Kawatani, T. Kanki, and H. Tanaka, Jpn. J. Appl. Phys., Part 1 50, 055804 (2011).
10) S. Sedky, P. Fiorini, M. Caymax, A. Verbist, and C. Baert, Sens. Actuators A 66, 193 (2003).
11) S. Eminoglu, D. S. Tezcan, M. Y. Tanrikulu, and T. Akin, Sens. Actuators A 109, 102 (2003).
12) M. Moreno, A. Kosarev, A. Torres, and R. Ambrosio, Thin Solid Films 515, 7607 (2007).
13) M. Nishikawa, T. Nakajima, T. Kumagai, T. Okutani, and T. Tsuchiya, J. Ceram. Soc. Jpn. 119, 577 (2011).
14) I. Takahashi, M. Hibino, and T. Kudo, Jpn. J. Appl. Phys., Part 1 40, 1391 (2004).
15) K. Miyazaki, K. Shibuya, M. Suzuki, H. Wado, and A. Sawa, Jpn. J. App. Phys., Part 1 53, 071102 (2014).
16) M. Soltani, M. Chaker, E. Haddad, R. V. Kruzelecky, and J. Margot, Appl. Phys. Lett. 85, 1958 (2004).
17) K. Miyazaki, K. Shibuya, M. Suzuki, H. Wado A. Sawa, J. Appl. Phys. 118, 055301 (2015).
18) J. P. Pouget and H. Launois, J. Phys. Colloq. 37, C4-49 (1976).
19) G. Villeneuve, A. Bordet, A. Casalot, J. P. Pouget, H. Launois, and P. Lederer, J. Phys. Chem. Solids 33, 1953 (1972).
20) M. Pan, H. M. Zhong, S. W. Wang, J. Liu, Z. F. Li, X. S. Chen, and W. Lu, J. Cryst. Growth 265, 121 (2004).
21) A. Sharoni, J. G. Ramírez, and I. K. Schuller, Phys. Rev. Lett. 101, 026404(2008).
22) H. Takami, T. Kanki, and H. Tanaka, Appl. Phys. Lett. 104, 023104 (2014).
23) J. B. Goodenough and H. Y.-P. Hong, Phys. Rev. B 8, 1323 (1973).

著者

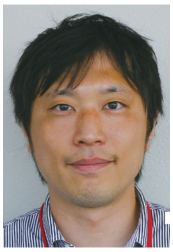

宮崎 憲一
みやざき けんいち

基礎研究２部
博士（工学）
半導体デバイスの研究開発に従事

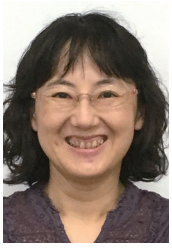

鈴木 愛美
すずき めぐみ

基礎研究２部
半導体デバイスの研究開発に従事

酒井 賢一
さかい けんいち

基礎研究２部
半導体デバイスの研究開発に従事

渋谷 圭介
しぶや けいすけ

（国研）産業技術総合研究所
博士（科学）
酸化物エレクトロニクスの研究に従事

澤 彰仁
さわ あきひと

（国研）産業技術総合研究所
博士（工学）
酸化物エレクトロニクスの研究に従事

藤田 淳一
ふじた じゅんいち

筑波大学数理物質系物理工学専攻教授，
応用理工学類学類長
博士（工学）
グラフェンを利用したエレクトロニクスの
研究に従事